

Anomalous Dispersion in Predictive Rendering

Andrea Weidlich¹ and Alexander Wilkie²

¹Vienna University of Technology, Austria

²Charles University in Prague, Czech Republic

Abstract

In coloured media, the index of refraction does not decrease monotonically with increasing wavelength, but behaves in a quite non-monotonical way. This behaviour is called anomalous dispersion and results from the fact that the absorption of a material influences its index of refraction.

So far, this interesting fact has not been widely acknowledged by the graphics community. In this paper, we demonstrate how to calculate the correct refractive index for a material based on its absorption spectrum with the Kramers-Kronig relation, and we discuss for which types of objects this effect is relevant in practice.

Categories and Subject Descriptors (according to ACM CCS): Computer Graphics [I.3.3]: Three-Dimensional Graphics and Realism—

1. Introduction

Dispersive refraction – the split of polychromatic light into its spectral components – is perhaps the simplest, but also one of the most visually prominent attributes of all transparent materials. Frequently included in computer graphics applications, the effect can be considered common knowledge in the graphics engineering community. However, most current graphics implementations of dispersive refraction use approximative formulas taken from optics, which implicitly assume that the index of refraction (IOR) always decreases towards shorter wavelengths. This is a valid assumption for colourless transparent solids; however, for *coloured* transparent objects, it often is not. For such objects, the IOR can exhibit a markedly non-monotonic behaviour. This behaviour is called *anomalous dispersion* in optics literature (in contrast to the *normal dispersion* found in plain transparent substances), and its most obvious consequence is a partial reversal of the usual sequence of prismatic colours (see figure 1 for an illustration).

Regions of anomalous dispersion always occur around absorption frequencies, because there is a direct connection between the IOR and the absorption of a material. This means that every substance has regions of normal and anomalous dispersion, because every real material has one or more bands of absorption. If at least one of them lies in the visible spectrum (which is the case for coloured dielectrics) the phenomenon of anomalous dispersion is visible.

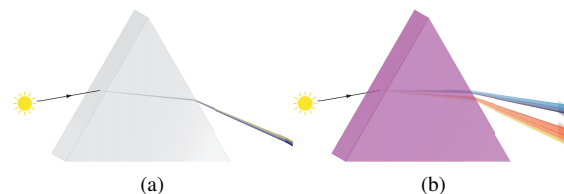


Figure 1: Dispersive refraction of light falling through prisms made of (a) clear BK7 glass, and (b) a Fuchsine solution. For the pink prism, the order of the spectral colours is reversed and the pattern is much larger, although the average IOR is approximately the same for both materials. The green part of the incident light is completely absorbed in (b).

In this paper we investigate the importance of this effect for computer graphics applications, and also show how one can include this effect in a ray-based renderer. Our goal is to make this particular area of optics knowledge accessible to computer graphics engineers, by giving a brief introduction into the relevant physical background, and by presenting a ready-to-use technique that computes the IOR from absorption data. Since the classical, simple dispersion formulas cannot be used to calculate this effect, we show how one can use the Kramers–Kronig relations to calculate the index of refraction from absorption data. We then demonstrate that

the effect of anomalous dispersion can really lead to visible artefacts in scenes that contain coloured dispersive objects, and also discuss when one can safely omit such calculations.

2. Background

While the connection between the absorption characteristics of an object and its IOR is well known to physicists, this fact has received hardly any attention in the graphics community so far, except for very recently [FCJ07], but even there, anomalous dispersion as such was not investigated. In [Fri08] the influence of the absorption on the reflection was discussed. The main reason why this connection is relevant for computer graphics is that the common modelling practice of choosing the IOR and colour of a transparent object independently of each other is physically incorrect, and can lead to visually detectible errors.

2.1. Dispersive Refraction

When light strikes an interface between two different media, some of the energy is reflected, propagates in the mirror direction and stays within the first medium. In most cases, a part of the incident energy also enters the second medium, and continues its propagation there. How large this second part is, and in which direction it continues its path, is dependent on the relative density of the two media; the speed of light is changed at the interface between the two, and (except at normal incidence) a change of direction occurs – the light is said to be refracted. The relationship between angle of incidence and angle of refraction of a light wave when travelling between two media with different refractive indices is given by Snell's law

$$n_1(\lambda) \sin \theta_1 = n_2(\lambda) \sin \theta_2 \quad (1)$$

where $n_1(\lambda)$ and $n_2(\lambda)$ are the respective, wavelength-dependent refractive indices, and θ_1 and θ_2 are the angles between normal and incident, and normal and refracted ray. Since the IOR of all transparent materials is not a constant, but depends on the wavelength, light of different wavelengths is deflected in slightly different directions, which produces an angular separation of the colours, called dispersion.

Strictly speaking, equation 1 is only valid for light that enters a perfectly transparent material. For all materials that do exhibit some form of attenuation when light passes through them, it is convenient to group information about the IOR and the attenuation characteristics into a single, complex-valued entity, the complex index of refraction $\tilde{n}(\lambda)$:

$$\tilde{n}(\lambda) = n(\lambda) + i k(\lambda), \quad (2)$$

where $n(\lambda)$ is the real-valued IOR from equation 1, and $k(\lambda)$ is referred to as the extinction coefficient (or, sometimes, the absorption index) of the material. k is given by

$$k(\lambda) = \frac{\lambda \alpha(\lambda)}{4\pi}, \quad (3)$$

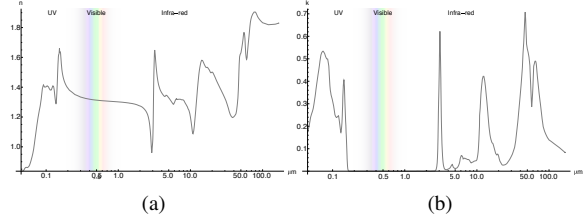


Figure 2: (a) n and (b) k of water ice from the UV to the far infra-red. Outside the visible range the index of refraction changes dramatically while it is smooth in the visible region, because no absorption occurs there. After [War84].

where $\alpha(\lambda)$ is the absorption coefficient that describes the absorbance $A(\lambda)$ of a medium with path length l .

$$A(\lambda) = \alpha(\lambda)l \quad (4)$$

It is worth noting that in principle, all materials can be described by a complex-valued IOR; perfectly transparent materials are simply assumed to have a $k(\lambda)$ of zero. In computer graphics, one usually only encounters $k(\lambda)$ when the Fresnel terms for strongly absorbing media (such as metals) have to be evaluated. But in fact all coloured, transparent objects have an IOR with a non-zero imaginary component, even though it is usually quite small for such materials.

2.2. Anomalous Dispersion of Light

For practically all colourless dielectrics, the IOR monotonically decreases for increasing wavelengths in the visible range, which means that the dispersive fan-out will be in the strict wavelength order one has grown accustomed to from rainbows of all sorts: from violet and blue via green to yellow, orange and red. However, even for objects that are completely transparent in the visual range, the refractive index is not monotonic everywhere.

In this context, it is instructive to examine an IOR plot that covers a wide range of wavelengths, such as figure 2, which shows the refractive behaviour of water ice from the UV to the far infra-red. Plots like that reveal that for all dielectric substances, the IOR only behaves monotonically in the regions between the absorption bands. In the immediate neighbourhood of the absorption band the IOR first starts to decrease strongly with increasing wavelength, then abruptly increases, and finally decreases to a normal level again.

The reason for this is as follows: when an electromagnetic wave encounters a collection of atoms, an oscillating electromagnetic field \mathbf{E} is superimposed on the field of forces that is responsible for the coherency of the material. As a result of this external force, the electrons in the material are forced to leave their equilibrium positions. One consequence of this is that the entire atom to which the displaced electron belongs turns into an electric dipole, and that the atom starts to

exhibit an electric polarisation \mathbf{P} [BW99].

$$\mathbf{P} = \epsilon_0 \chi \mathbf{E} \quad (5)$$

where ϵ_0 is the electric permittivity and χ is the electric susceptibility. This electron displacement grows larger as the excitation frequency moves closer to one of the characteristic resonance frequencies ω_o of the material. As long as the excitation frequency is *smaller* than the resonance frequency, the excited and the forced oscillation of individual dipoles are in phase, and the dipoles can respond to the excitation. At the actual resonance frequency, energy can be transferred to the system with very little resistance. The amplitude of the resulting oscillations becomes very large – much larger than the amplitude of the driving force, as the light can travel with low resistance, and the IOR decreases rapidly. Once the excitation frequency is *larger* than the resonance frequency, though, excitation and oscillation of the dipoles are suddenly 180° out of phase. The dipoles are no longer able to properly react to incident oscillations that are now too fast for them, and energy can only be transferred to the system by overcoming a significantly higher resistance. Consequently, light suddenly travels much slower, and the IOR increases significantly once the frequency of incident light has moved past the absorption frequency. Once the incident frequency moves further away from the absorption frequency, this effect gradually wears off, and normal, undisturbed propagation in the material resumes.

All this leads us to the somewhat surprising conclusions that (a) even for the simple case of colourless dielectrics, the dispersion behavior of the material in the visible range is actually directly determined by the location and intensity of the absorption bands that the substance exhibits in the regions of the electromagnetic spectrum *adjacent* to the visible range and (b) that all materials have regions of normal and anomalous dispersion, because apart from the limit case of vacuum, one or more strong absorption bands can be found in every real material. The effect becomes directly visible (and thereby relevant for computer graphics) if one or more absorption bands lie in the visible region.

3. Kramers-Kronig Relations

Since the classical dispersion formulas implicitly assume the IOR to be monotonically falling, they cannot be used if the material has one or more absorption bands in the visible part of the spectrum, i.e. if the material is not colourless. Tables with measured IOR data are a rarity in literature, so an analytical approach is needed. Fortunately, there is a direct connection between the IOR and the absorption characteristics of a material, and it is possible to calculate one from the other using the Kramers–Kronig relations (KKR).

3.1. Kramers–Kronig Relations for the IOR

In physics, the Kramers–Kronig relations (KKR) are a well known tool that, given one component of a meromorphic

complex-valued function, can be used to determine the other component. In our case this means we can calculate the real-valued IOR from the imaginary extinction coefficient.

The reason for this is one of the most fundamental notions in physics: the *principle of causality* – a system cannot respond before an excitation has actually taken place. It also holds for light-object interactions. Matter is excited by the electric field of the incident beam, which forces the dipoles of the material to vibrate, and the material responds with polarisation. The electric charges become the source of an electromagnetic wave which results in reflected and transmitted beams of light (Huygens’ principle). If the field varies with time, so does the polarisation, whereas \mathbf{P} is proportional to \mathbf{E} . Equation 5 can be written as a response function.

$$\mathbf{P}(t) = \epsilon_0 \int_{-\infty}^{\infty} \mathbf{E}(t') \bar{\chi}(t-t') dt' \quad (6)$$

Equation 9 is a time-dependent function $\bar{a}(t)$ with $\bar{a}(t) = 0$ for $t < 0$. The principle of causality guarantees that for the Fourier transform $a(\omega)$ of $\bar{a}(t)$ the real and imaginary components are Hilbert transforms of each other, so that the Fourier transform of $\chi(\omega)$ of the susceptibility $\bar{\chi}(t)$ can be written as [LPSV05]

$$\text{Re}\{\chi(\omega)\} = \frac{2}{\pi} \mathcal{P} \int_0^{\infty} \frac{\omega' \text{Im}\{\chi(\omega')\}}{\omega'^2 - \omega^2} d\omega' \quad (7)$$

$$\text{Im}\{\chi(\omega)\} = -\frac{2\omega}{\pi} \mathcal{P} \int_0^{\infty} \frac{\text{Re}\{\chi(\omega')\}}{\omega'^2 - \omega^2} d\omega' \quad (8)$$

where \mathcal{P} denotes the principal value of the integral. Since

$$\sqrt{1 + 4\pi\chi(\omega)} = n(\omega) + ik(\omega) \quad (9)$$

is holomorphic in the upper complex ω -plane, equation 7 and 8 can be rewritten in a form that it connects the real and imaginary parts of the frequency-dependent complex-valued refractive index $\tilde{n}(\omega)$ [LPSV05]

$$n(\omega) = 1 + \frac{2}{\pi} \mathcal{P} \int_0^{\infty} \frac{\omega' k(\omega')}{\omega'^2 - \omega^2} d\omega' \quad (10)$$

$$k(\omega) = -\frac{2\omega}{\pi} \mathcal{P} \int_0^{\infty} \frac{n(\omega') - 1}{\omega'^2 - \omega^2} d\omega' \quad (11)$$

These relations are called the Kramers-Kronig relations; the structure of this relationship is derived from mathematical considerations alone. If used in the optical context discussed above, ω' can take on the meaning of the frequency for which the frequency-dependent resonance behaviour of the material is being evaluated. In physics literature the KKR are normally given in terms of angular frequency ω , and for an integration range of $[0, \infty]$. For our purposes it is more convenient to rewrite them in terms of wavelength λ , and for a given, finite integration range $[\lambda'_{min}, \lambda'_{max}]$; the latter is necessary because absorption data is usually not available for the entire frequency range [WO03].

$$n(\lambda) = n_b + \frac{2\lambda^2}{\pi} \mathcal{P} \int_{\lambda'_{max}}^{\lambda'_{min}} \frac{k(\lambda')}{\lambda'(\lambda^2 - \lambda'^2)} d\lambda' \quad (12)$$

n_b is the background refractive index.

3.2. Solving the Kramers–Kronig Relation

There are two potential problems which limit the practical usefulness of the KKR:

- An analytical solution for equation 10 would require absorption data over the range $[0, \infty]$. This is clearly impractical for use in computer graphics, since one usually only has absorption data for a small part of the entire frequency range, such as the visible spectrum, available.
- The integral has a pole at $\lambda^2 - \lambda'^2$. This pole requires an approximation.

In practice, this means one has to extrapolate the absorbance values beyond the actual measurement data and perform the numerical integration by using a specific numeric integration formula on the KKR integrals that can handle the pole $\lambda^2 - \lambda'^2$. In the following two sections, we describe each of these tasks in more detail.

3.2.1. Dealing With Measurement Data Taken Over a Finite Range

Since absorption data cannot be measured over the complete spectral domain with reasonable effort, one has to decide what to do with the limited data. One strategy is to extrapolate the data outside the measured range by defining a physical model which corresponds to the optical property under investigation (usually a Gauss distribution is used to simulate an absorption band). A different approach is to directly use the limited experimental data that is available, without attempting any extrapolation. This strategy is expected to be successful only when the optical property in question falls off quickly outside the measured spectral range, and remains at zero for all frequencies outside the measured range.

3.2.2. Performing the Integration

The problem of how to perform the actual integration in the presence of a pole in the function is of a numerical nature, and a moderate amount of literature exists on how one can tackle such an issue. One possibility is the use of Fourier transforms [Kin07]. A different, rather straight-forward and accurate method to solve the KKR is the use of Maclaurin's Formula since it is very easy and also accurate [OI88]; this is the technique we resorted to.

If the values of an absorption spectrum $k(\lambda)$ are transformed and stored as m discrete values

$$k(\lambda)_1, k(\lambda)_2, k(\lambda)_3, \dots, k(\lambda)_j, \dots, k(\lambda)_{m-1}, k(\lambda)_m \quad (13)$$

and

$$h = \lambda_{j+1} - \lambda_j \text{ for } (j = 1, 2, \dots, m - 1) \quad (14)$$

is the integration interval, we can approximate the estimate of the integral by taking every other point into account so that

$$I_i = \frac{2\lambda^2}{\pi} \times 2h \times \left\{ \sum_j' f_j \right\} \quad (15)$$

where

$$f_j = \frac{k(\lambda')}{\lambda'(\lambda^2 - \lambda'^2)} \quad (16)$$

The \sum_j' denotes that if i is odd, $j = 2, 4, 6, \dots, i - 1, i + 1, \dots$, and if i is even, $j = 1, 3, 5, \dots, i - 1, i + 1, \dots$. This way we can avoid a calculation of the pole at $i = j$. Mathematica® code that shows how this formula can be used to calculate the IOR from the extinction coefficient in practice can be found in appendix A.

Generally, the error incurred by truncating the function outside the visual range is quite small, which, given the inherently rather local influence of each component on the other, is not entirely surprising. However, an exact assessment of the truncation error is also possible and can be found in [LPSV05]. A discussion of the error that arises though the use of Maclaurin's Formula can be found in [OI88]. These issues should always be kept in mind when performing anomalous dispersion calculations based on absorbance data, in particular if highly accurate results are desired.

4. Results

4.1. Integration of Dispersion into a Ray-based Renderer

The simulation of normal dispersion has been addressed numerous times in computer graphics. It was first introduced to computer graphics by [Tho86] as an add-on to a standard ray tracer that breaks up the incident energy into six subrays, where each one represented only a part of the spectrum. [YKIS88] managed to reduce the computational complexity by using only three rays to represent a spreading incident ray. Dispersion was further investigated by [SFD00b], who used a hybrid spectral model which decomposed the spectrum into its smooth component, and a collection of spikes to optimally represent monochromatic light rays and spiky emission spectra to render dispersion in gemstones, later also in combination with absorption [SFD99]. [GS04] presented an integrated real-time system capable of interactively rendering gemstones including dispersion effects.

We decided to use a stratified sampling approach similar to that of [SFD00a]; a polychrome ray is split up into a fixed number of monochrome sub-rays on the first dispersive interface, which are then followed individually through the scene without any further path forking. The wavelength of each sub-ray is chosen stochastically from the spectrum that was first partitioned into as many segments as sub-rays will be generated in each step. We used 45 sub-rays; comparisons with 450 showed no visually detectable differences. We choose this approach because is straight-forward to implement. Also, a more sophisticated approach that chooses the number of samples according to the dispersion value of the material could be counterproductive in this scenario due to the anomalous behaviour of the IOR.

Although the realisation of dispersion is possible in a tristimulus based rendering system, it does not yield good results due to the limited number of colours and the resulting low quality rainbow effects. For this reason we used the Advanced Rendering Toolkit (ART), a spectral rendering research system, as our implementation testbed, instead of a conventional RGB colour space rendering system.

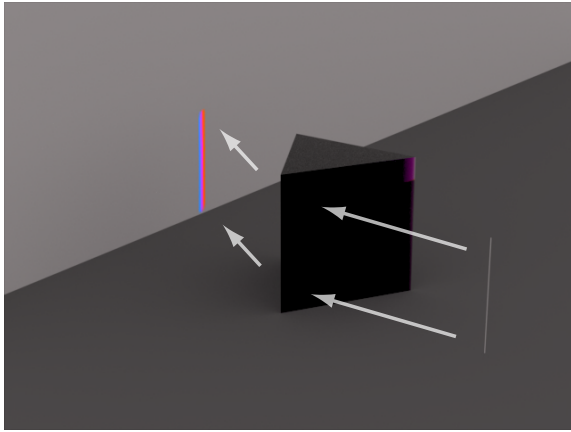


Figure 3: An overview rendering of the scene geometry we used to demonstrate the effect. The white arrows show the approximate optical path that caused the rainbow pattern in this image. Figure 5 shows close-up images of these rainbow patterns for various prism materials.

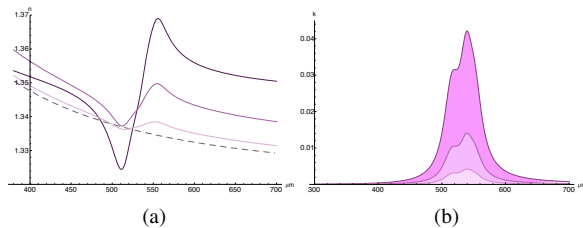


Figure 4: (a) n and (b) k for rose bengal solutions of varying concentration. The three curves correspond to the dispersion patterns shown in the top row of figure 5 – dark pink for image 5a (high concentration), medium pink for 5c (medium concentration), and bright pink for 5e (weak concentration). The dotted line in (a) is the IOR of pure water.

4.2. Rendering of Anomalous Dispersion Effects

The characteristic partial reversal of the colour sequence in a rainbow that results from the anomalous behaviour of the refractive index is occasionally mentioned in physics literature, sometimes even schematically sketched (e.g. [Ber93] or [Nas01]). However, actual photos of the effect are quite rare, since it is difficult to observe in an experimental setting. This lies in the nature of the phenomenon; the effect is most

prominent exactly in those wavelength regions where the absorption of light is strongest. Nonetheless, there are several ways to make this effect visible. The first person who observed and analysed anomalous dispersion was [Chr71] by using an alcohol Fuchsine solution of 19 percent and a prism with a very small refractive angle of $1^\circ 14'$. Later [Kun71] and [Pfi98] as well as [Woo99] [WM01] further examined techniques to make anomalous dispersion visible and measured the change in the index of refraction. A complete review of the known techniques to observe anomalous dispersion can be found in [EHB98] where also a photo of the effect can be seen.

The most striking demonstration of the phenomenon is that if one uses a strongly coloured prism to split a light ray into its rainbow components, the order of the rainbow colours will be partially reversed in some regions of the spectrum. So after establishing the theoretical foundations outlined in the previous sections, our next goal was to reproduce the effect in various renderings, in order to properly assess its importance for computer graphics.

To demonstrate the effect, we first performed this experiment; an overview is shown in figure 3. As material properties for the prism we assumed those of rose bengal diluted in water, and used the extinction coefficient and IOR data provided by [van15] as input. We performed our virtual optical experiment with a prism being made up from three solutions of rose bengal with different concentration; a strongly dyed 10 percent solution, a less concentrated 3.3 percent solution and a 1 percent solution of the same substance. The indices of refraction and the extinction coefficients can be seen in figure 4 for all concentrations. The same prisms were also rendered with the IOR of pure water to see what happens if the influence of the extinction coefficient is neglected.

Just like in the classical experimental setup for this phenomenon, a directional light source was placed at the thin edge of the coloured prism so that the incident rays are already split into their prismatic colours, but the absorption is still weak. The result was as expected and in accordance with the photo that can be seen in [EHB98] – the colors are separated and reversed, since the anomalous change in the refractive index is very strong in this case (figure 5a). Two things can be observed:

- The colour sequence goes from indigo to blue and violet, is followed by red through orange to yellow. Green is absorbed completely. However, there is no clear separation between blue and violet, because some wavelengths have the same index of refraction, and therefore some colours that are normally separated are mixed together.
- The dispersive fan-out is much wider for anomalous dispersion, than for a pure water solution in the same geometrical setting (figure 5b).

However, once we moved the light source towards the thicker part of the prism, the dispersion pattern soon van-

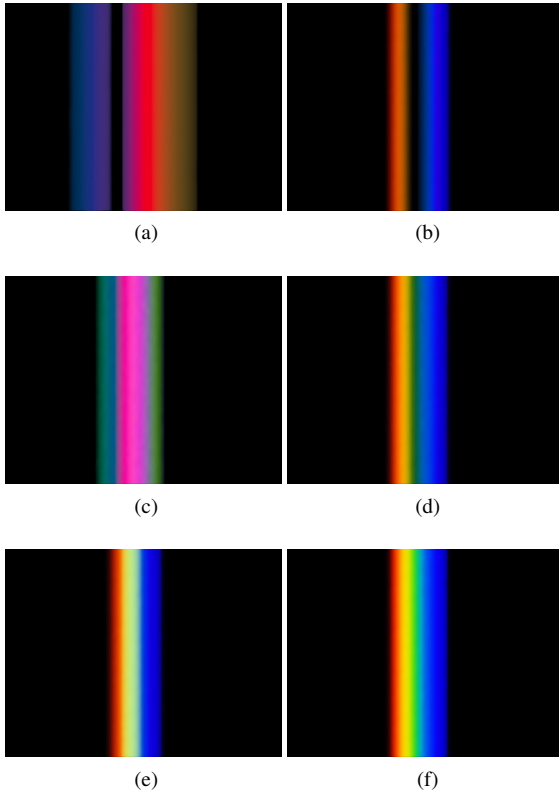


Figure 5: Dispersion patterns created by light falling through a prism filled with – from top to bottom – decreasing concentrations of rose bengal, diluted in water (left column), and patterns created by light falling through prisms with exactly the same transmission characteristics, but with the IOR of plain water where the order of the rainbow colours stays the same (right column).

ished, because all light is swallowed by the much stronger absorption.

The dispersion curve of the second solution with decreased concentration also exhibited some anomalous behaviour, but not as strongly as in the first experiment (figure 5c). Still, compared to rendered images that use just a normal dispersion curve, a difference can be seen, even if the light source is moved away from the edge and the absorption becomes stronger.

The anomalous behavior of the dispersion becomes even weaker for the third solution (figure 5e). There is only a small region of anomalous behaviour and only the colours between 480 and 570 nm are mixed together; the visual difference is only marginal otherwise, and the colour sequence is similar to the dispersion pattern of pure water (figure 5f).

If done with a real tinted solution in a lab setting, the experiment is allegedly hard to get right, since controlling the

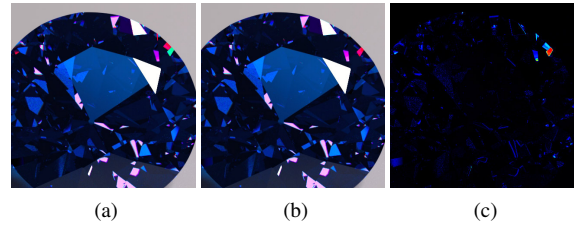


Figure 6: Comparison of a strongly coloured, brilliant cut gemstone of 1mm size, rendered (a) with and (b) without anomalous dispersion effects and a difference image (c).

dilution of the coloured solution requires care, and hollow prism of quite specific shape is needed. Unsurprisingly, the experiment proved to be very simple to set up in its simulated form by comparison.

4.3. Anomalous Dispersion in Crystals

After the experiment discussed in the previous section had shown that, at least in principle, there are certain materials and situations where anomalous dispersion cannot be neglected if truly accurate rendering is desired. We wanted to focus on the one application where this phenomenon might make a difference that is large enough to warrant its consideration in production rendering systems – the area of gemstone rendering. Coloured, transparent cut gemstones such as sapphires, rubies and emeralds all obviously owe their colour to absorption bands in the visible range, and therefore ought to exhibit the phenomenon to some degree.

In order to determine whether the inclusion of the effect causes visually detectable differences in the appearance of rendered gemstones, we performed two experiments. In each of these, we rendered a gemstone with and without anomalous dispersion, and compared the differences. The two test cases were a strongly coloured brilliant cut blue spinel, and an intensively coloured pink gemstone that we rendered in four different sizes. As with the rose bengal prism, we did not want to use artificial data for the absorption characteristics of the gemstone. We wanted to examine the influence of the effect on a real gemstone, so we used the data of [Tro34]. He measured the IOR and the absorption of several different types of spinel, which clearly illustrate the change from normal to anomalous dispersion with increasing absorption. Since the absorption data is only given in galvanometer readings, we used the KKR to calculate the extinction coefficient from the IOR for the visible spectrum.

As can be seen in figure 6, the results of this experiment are at best ambiguous although a few differences are visible – a few of the colourful dispersion “flashes” that can be seen on the crown are different. For this case, one can conclude that anomalous dispersion only has to be included if perfect pixel-by-pixel accuracy of renderings of such a stone

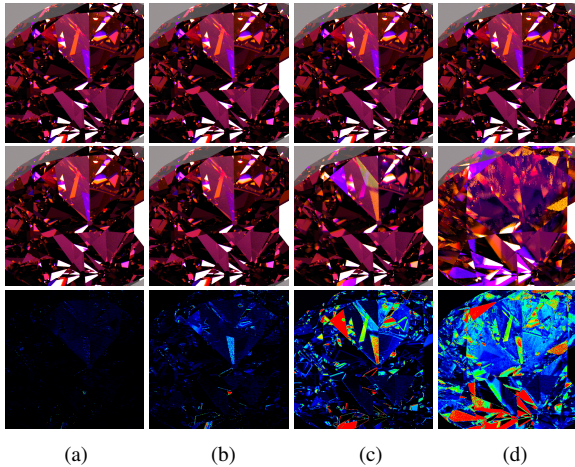


Figure 7: A brilliant cut gemstone with the basic dispersion characteristics of diamond, and a single strong region of absorption in the green region of the spectrum. The top row are images rendered with a naive, physically incorrect IOR, the next row shows the results if anomalous dispersion is taken into account, and the last row are difference images.

is desired. For all other applications, the normal IOR of an un-coloured stone is apparently sufficient.

However, the situation is different for smaller objects. We rendered four different brilliant cut gemstones with the same overall transparency and colour (figure 7). The difference between the four cases is the size of the stone: (a) shows a stone with a diameter of 1cm, (b) of 1mm, (c) 0.1mm, and (d) 0.01mm. The absorption was scaled so that all four stones have similar overall appearance; this means that the minuscule stone used for case (d) is made from a *much* more opaque material than the one shown in (a). (a) has the absorption characteristics of a pink diamond; for the remaining stones we increased its absorbance, i.e. the data for the stones in (b) to (d) is artificial – but still plausible – and we used the KKR to calculate the corresponding IOR. Cases (c) and (d) exhibit significant changes, although the effect does cause some smaller differences even for case (b).

4.3.1. Coatings

Due to the minuscule size of the smallest of the four test objects, this feature probably still does not make anomalous dispersion particularly relevant for actual renderings of macroscopic objects, except perhaps for tiny crystals at very large magnifications. However, as can be seen from the large visual differences in the third and fourth cases shown in figure 7, the dispersion behaviour of small structures made of strongly absorbent material is indeed very susceptible to changes due to anomalous dispersion. Which makes the phenomenon very relevant for all simulations that involve small structures that contain strongly absorbent materials, such as



Figure 8: Spheres coated with three different effect lacquers of the type described by [SMAS08], without (left half of images) and with (right half) anomalous dispersion of the pigment particles taken into account. Apart from the dispersion characteristics of the pigments, the BRDF parameters (and in particular, the absorption characteristics of the pigment particles) are identical.

complex, layered BRDFs or pigments that can be found in cosmetic products, with an appearance that is partly determined by the inclusion of such particles [SMAS08] or the prediction of the appearance of fibers from e.g. woven fabrics [RKS97].

To demonstrate the former point, we rendered three spheres coated with an effect lacquer that derives its appearance from very small, strongly absorbing particles that are supported in a binder matrix. We used the model similar to that proposed by [SMAS08]; the particles are non-spherical, and oriented randomly according to a Gaussian distribution. The transfer matrix method was used to compute the actual reflectance values, and the material parameters were those of actual substances used in such coatings. The parameter values were taken from literature, e.g. for mica covered with titanium dioxide that is again covered by iron oxide particles (one of our test cases).

As can be seen in figure 8, the difference in chroma between a simulation that considers anomalous dispersion, and one that does not, is quite strong. Also, the goniochromic behaviour of the BRDF is obviously also altered by the inclusion of this effect, as can be best seen on the leftmost sphere. This example illustrates that the common practice in contemporary computer graphics to neglect anomalous IOR behaviour in lacquer models that include pigments is a potentially major source of error.

5. Conclusion and Future Work

In this paper we have shown the following three main points:

1. How one can, for a given material absorbance, compute the correct changes that have to be made to the index of refraction compared to a similar transparent material,
2. that the effect of anomalous dispersion is not particularly relevant for normal-sized objects, except if utmost accuracy is desired, but we also showed
3. that the effect can cause large deviations from normal refractive behaviour if the objects in question are very small

or thin, and made from strongly absorbent materials; this includes strongly absorbent particles in complex BRDFs.

Future work in this area will include further investigations of scenarios that might require anomalous dispersion capabilities for accurate prediction of their appearance. Candidates for such scenarios are woven materials made from thin, strongly absorbent fibers, certain types of crystalline surface coatings, and specialised forms of effect paintwork that include small, non-metallic, and strongly absorbing particles like e.g. dyes to achieve their appearance.

Appendix A: Calculating the IOR from absorbance values

This code shows how the KKR can be used to calculate the IOR from the extinction coefficient. There are two input parameters: the first is a two-dimensional list with n elements $s[\{\{\lambda_n, k_n\}\}]$; the first component of each element contains the wavelength, and the second the extinction coefficient at this wavelength. The second is a one-dimensional list $nb[\{n_n\}]$ that stores the basic IOR.

```

maclaurinN[s_, nb_] := Module[
  { m, mm, k, v, i, j },
  m = 84; (* number of sample points *)
  mm = (720-300)/m; (* Distance between sample points *)

  fOdd[i_]:=
    Sum[ s[[j]][[2]] / (s[[j]][[1]]*s[[i]][[1]]2 - s[[j]][[1]]2 ),
      {j, 2, m, 2}];
  fEven[i_]:=
    Sum[ s[[j]][[2]] / (s[[j]][[1]]*(s[[i]][[1]]2 - s[[j]][[1]]2 )),
      {j, 1, m, 2}];

  f[i_] := If[ Mod[i, 2] == 0, fEven[i], fOdd[i] ];

  maclaurin[i_, h_] := (2*s[[i]][[1]]2) /  $\pi$  * 2h*f[i];
  n = Table[{300 +  $\lambda$ *mm,
    nb[300 +  $\lambda$ *mm] + maclaurin[ $\lambda$ , mm] }, { $\lambda$ , m} ] ]

```

References

[Ber93] BERGMANN L.: *Optik*, vol. 3 of *Lehrbuch der Experimentalphysik*. de Gruyter, 1993.

[BW99] BORN M., WOLF E.: *Principles of Optics. Electromagnetic Theory of Propagation, Interference and Diffraction of Light*, 7 ed. Cambridge University Press, Cambridge, 1999.

[Chr71] CHRISTIANSEN C.: Über das Brechungsverhältniss des Fuchsins. *Annalen der Physik* 219 (1871), 250–259.

[EHB98] ERDÉLYI M., HILBERT M., BOR Z.: Anomalous dispersion of dye solutions observed in a prismatic cuvette. *American Journal of Physics* 66 (Sept. 1998), 791–793.

[FCJ07] FRISVAD J. R., CHRISTENSEN N. J., JENSEN H. W.: Computing the scattering properties of participating media using lorenz-mie theory. *ACM Trans. Graph.* 26, 3 (2007), 60.

[Fri08] FRISVAD J. R.: *Light, Matter, and Geometry : The Cornerstones of Appearance Modelling*. VDM Verlag Dr. Müller, 2008.

[GS04] GUY S., SOLER C.: Graphics gems revisited. *ACM Transactions on Graphics (Proceedings of the SIGGRAPH conference)* 23, 3 (2004), 231–238.

[Kin07] KING F. W.: Numerical evaluation of truncated kramers-kronig transforms. *J. Opt. Soc. Am. B* 24, 7 (2007), 1589–1595.

[Kun71] KUNDT A.: Über anomale Dispersion. *Annalen der Physik* 220 (1871), 128–137.

[LPSV05] LUCARINI V., PEIPONEN K.-E., SAARINEN J. J., VARTIAINEN E. M.: *Kramers-Kronig Relations in Optical Materials Research*. Springer, Berlin Heidelberg, 2005.

[Nas01] NASSAU K.: *The Physics and Chemistry of Color*, 2 ed. John Wiley & Sons, Inc., United States, 2001.

[OI88] OHTA K., ISHIDA H.: Comparison among several numerical integration methods for Kramers-Kronig transformation. *Applied Spectroscopy* 42 (Aug 1988), 952.

[Pfl98] PFLÜGER A.: Prüfung der Ketteler-Helmholtz'schen Dispersionsformeln an den optischen Constanten anomal dispergirender, fester Farbstoffe. *Annalen der Physik* 301 (Jan 1898), 173–213.

[RKS97] RUBIN B., KOBZA H., SHEARER S. M.: Prediction and verification of an iridescent synthetic fiber. *Appl. Opt.* 36, 25 (1997), 6388–6392.

[SFD99] SUN Y., FRACCHIA F. D., DREW M. S.: Rendering the phenomena of volume absorption in homogeneous transparent materials. In *2nd Annual IASTED International Conference on Computer Graphics and Imaging (CGIM '99)* (1999), pp. 283–288.

[SFD00a] SUN Y., FRACCHIA F., DREW M.: Rendering diamonds. In *Proceedings of the 11th Western Computer Graphics Symposium (WCGS)* (2000), pp. 9–15.

[SFD00b] SUN Y., FRACCHIA F. D., DREW M. S.: Rendering light dispersion with a composite spectral model. In *1st International Conference on Color in Graphics and Image Processing* (Nov. 2000), pp. 51–56.

[SMAS08] SHIOMI H., MISAKI E., ADACHI M., SUZUKI F.: High chroma pearlescent pigments designed by optical simulation. *Journal of Coatings Technology and Research* 5, 4 (Dec. 2008), 455–464.

[Tho86] THOMAS S. W.: Dispersive refraction in ray tracing. *The Visual Computer* 2, 1 (Jan. 1986), 3–8.

[Tro34] TROMNAU H.-W.: Chemische und physikalische untersuchungen an synthetischen mit kobalt gefärbten spinellen. *Neues Jahrbuch für Mineralogie, Geologie und Paläontologie, Beil-Bd* 68 (1934), 349–376.

[van15] VAN DER PLAATS B. J.: Untersuchung über Absorption und Dispersion des Lichtes in Farbstofflösungen. *Annalen der Physik* 352 (1915), 429–462.

[War84] WARREN S. G.: Optical constants of ice from the ultraviolet to the microwave. *Applied Optics* 23, 8 (1984), 1206–1225.

[WM01] WOOD R., MAGNUSON C.: The anomalous dispersion of cyanin. *Philos Mag* 1 (Jan 1901), 36–45.

[WO03] WAKAMATSU T., ODAUCHI S.: Thermal-changeable complex-refractive-index spectra of merocyanine aggregate films. *Appl. Opt.* 42, 34 (2003), 6929–6933.

[Woo99] WOOD R.: On cyanine prisms and a new method of exhibiting anomalous dispersion. *Proceedings of the Physical Society of London* 1 (Jan 1899), 671–674.

[YKIS88] YUAN Y., KUNII T. L., INAMOTO N., SUN L.: Gemstone fire: adaptive dispersive ray tracing of polyhedrons. *The Visual Computer* 4, 5 (1988), 259–270.